

Controlled drying to enhance properties of technical ceramics

Rajnish Misra*, Andrew J. Barker¹, James East

IRC in Materials for High Performance Applications, School of Chemical Engineering, University of Birmingham, Edgbaston, Birmingham B15 2TT, UK

Abstract

The drying kinetics of several technical ceramics such as alumina, boehmite and lead zirconate titanate (PZT) have been determined in order to maximise significant properties relative to their use for fuel cell tubes, catalyst supports and as components in hydrophones and multi-phase actuators. Common to all materials investigated is the need to avoid macro-cracking within the green ceramic precursor prior to sintering. Avoidance of this problem is achieved by optimising the temperature and relative humidity conditions for drying. Such controlled drying permits shrinkage to occur without the development of any gross macro-cracking, as evidenced by the examination of the microstructure of sintered materials. The experimental work that has established the utility of controlled drying as an essential step in producing high quality ceramics has involved the detailed analysis of drying rate data and its correlation with shrinkage which has been monitored using digital camera imaging. Such an understanding of the drying process will contribute to the production of a wide range of high quality defect-free ceramic components by the most cost-effective route. © 2002 Elsevier Science B.V. All rights reserved.

Keywords: Digital camera imaging; Drying kinetics; Macro-cracking; Poling; Shrinkage; Weibull modulus

1. Introduction

Alumina, boehmite and lead zirconate titanate (PZT) are all currently being utilised in order to fulfil a range of demanding applications within the fields of catalysis, electronics, energy production and structural component manufacture. These applications exploit rapid production techniques such as extrusion, twin-roll milling and injection moulding in order to achieve high volume output or a precision product of complex geometry. A major exigency for such high performance applications is the avoidance of macro-cracking which if successfully achieved will also lead to consistent strength of low variability.

Alumina has been established as a major constituent within the domain of ceramic material development, and as a result has been studied with respect to its sintering behaviour, mechanical properties, composite capabilities and, on a more limited scale, drying characteristics [1]. Thus, alumina was selected as a well-researched material which required further investigation with respect to drying characteristics and corresponding mechanical property development.

Boehmite, a precursor of alumina, is presently being used for demanding applications such as catalyst supports and fuel cell tube advancements, yet it has received limited attention

with respect to its drying characteristics [2]. It was therefore both opportune and appropriate to investigate the drying characteristics of boehmite paste over a range of drying conditions.

Applications involving the PZT as a piezoelectric material include geophones and multi-phase actuators [3]. The microstructure of PZT required for successful poling entails a high quality flaw-free component. It was therefore decided that an investigation into the drying characteristics of PZT should be performed in order to determine whether a superior microstructure could be achieved post-sintering.

2. Experimental

2.1. Materials preparation

In order to evaluate the properties of the ceramics, the precursors were prepared and extruded as cylindrical rods using a computer-controlled Instron load frame.

The alumina BAX 541 powder (supplied by Alcan Chemicals, Europe) was mixed with celacol B2/15 and de-ionised water in a Werner and Pfleiderer high shear mixer. In order to attain alumina paste batches of constant rheological properties, the overall mixing time was maintained constant, and the same mixing regime was followed for each batch preparation. Extrusion of the alumina paste as cylindrical rods was carried out at a ram speed of 1.0 mm/min through a 6.5 mm diameter die.

* Corresponding author. Tel.: +44-121-414-5289;
fax: +44-121-414-5324.

E-mail addresses: rajnishmisra@hotmail.com (R. Misra),
a.j.barker@bham.ac.uk (A.J. Barker).

¹ Co-corresponding author.

Nomenclature

d	diameter of sample (m)
l	length of sample (m)
m	normalised drying rate ($\text{kg}/\text{m}^2 \text{ s}$)
P	probability of failure (–)
t	time (s)
T	temperature ($^{\circ}\text{C}$)
X	moisture content, dry basis (–)
v	convective air flow velocity (m/s)

Greek symbols

ρ	density (kg/m^3)
σ	average bending strength (Pa)

Subscripts

av	average
c	critical
d	drying
dry	dry-bulb thermometer
o	original
sint	sintered
theo	theoretical
wet	wet-bulb thermometer

The boehmite PURAL SB1 powder (supplied by CON-DEA Chemie GmbH, Germany) was mixed with de-ionised water and aqueous nitric acid (1 wt.%) in a laboratory scale high shear kneader. Once again, constant mixing regimes

were followed in order to attain boehmite paste batches consisting of constant rheological properties. Extrusion of the boehmite paste as a cylindrical rod was performed at a ram speed of 2.0 mm/min through a 3.0 mm diameter die.

The commercial PZT 5A powder (supplied by Morgan Matroc, UK) was mixed in a beaker with PVA, methyl-cellulose, de-ionised water and glycerol. PZT sheets of a 2.5 mm thickness were produced by twin-roll milling the paste mix. The PZT paste system was found to be very stiff, thus extrusion of cylindrical rods was performed at 1.0 mm/min through a 3.0 mm diameter die.

Once extruded, all the rods were cut to 100 mm length and then rapidly transferred in air-tight containers to the drying cabinet in order to limit moisture loss to the ambient laboratory surroundings. In all the cases, at least 35 rods of defined dimensions were extruded and then dried. It was observed that even when simultaneously drying such a large number of samples within the environmental cabinet, the drying conditions of temperature and relative humidity remained constant.

2.2. Drying apparatus

The non-intrusive drying apparatus used to dry the monolithic ceramic rods (Fig. 1) enabled the real time online monitoring of sample weight loss, shrinkage and core temperature measurements during the drying process.

Under equilibrium conditions, a predetermined constant level of relative humidity (RH) was maintained within the environmental cabinet by the use of appropriate saturated

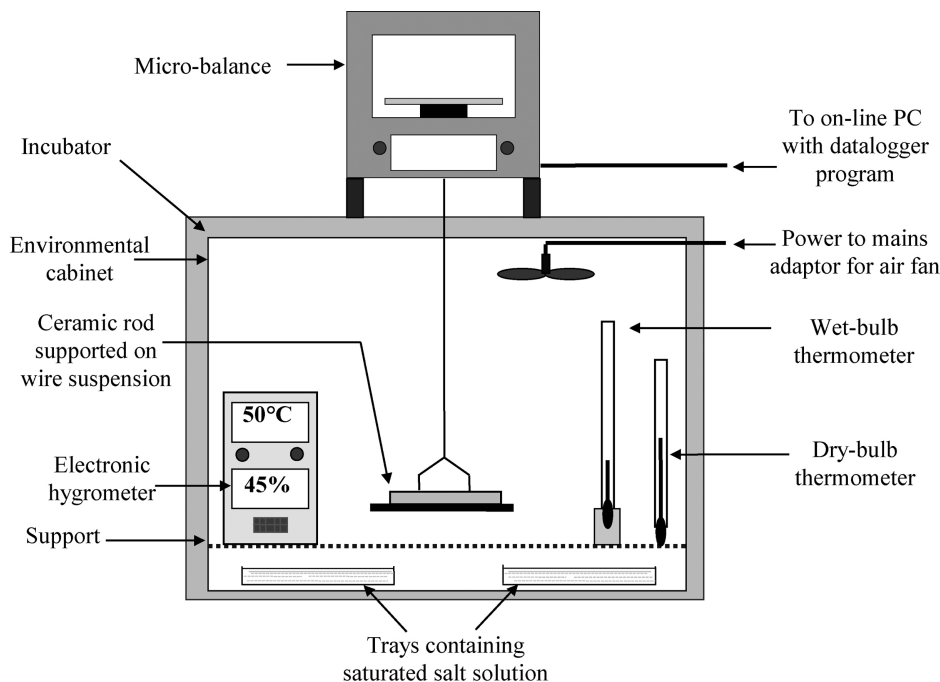


Fig. 1. Front view illustration of the non-intrusive drying cabinet (not to scale).

salt solutions: for example, LiCl (21–34% RH), K_2CO_3 (50–53% RH) and NaCl (78–86% RH). The wet- and dry-bulb thermometers, coupled with psychrometric tables, were used to ascertain the actual RH level. An additional electronic hygrometer was used in order to verify the dry-bulb thermometer temperature and humidity level.

A speed-controlled fan, positioned at the top of the environmental cabinet, provided a forced convective air flow across the ceramic specimen during drying. The air flow velocity perpendicular to the specimen was measured using an electronic anemometer.

A second sample (not illustrated in Fig. 1), heated at a geometrically similar position to the first sample within the environmental cabinet, was used to monitor the sample core temperatures by the use of K-type (Ni–Cr/Ni–Al) thermocouples connected to a datalogger which was also interfaced to the online computer.

2.3. Shrinkage measurements

The ceramic specimen shrinkage was monitored using a travelling microscope, and also for the purposes of comparison, a digital camera was both positioned outside the glass door in front of the environmental cabinet.

All of the drying experiments were conducted over a 27 h period. Within this period of time, the specimens' shrinkage ceased, and their core temperatures rose to the dry-bulb thermometer temperature, thus indicating that specimens had achieved equilibrium moisture contents.

2.4. Sintering regimes, mechanical testing and density measurements

After drying, the ceramic samples were heated at 110 °C for 12 h. This was necessary in order to determine the 'dry-bone weight' of the sample. All the dried samples were then sintered in a Lenton furnace. The alumina and boehmite rods were sintered at 1550 °C for 1 h, whilst the PZT rods were sintered at 1000 °C for 2 h.

Mechanical testing was performed using a computer-controlled Instron load frame fitted with three-point bend test equipment. A minimum of 35 rods were tested per material batch in order to obtain a statistically satisfactory estimate of bending strength and Weibull modulus.

Density measurements were achieved using the density bottle technique. The density of 10 samples was measured and then averaged in order to gain a final mean value for each material.

3. Results and discussion

In general terms, the differing drying characteristics of the ceramic precursors investigated may be attributed to a

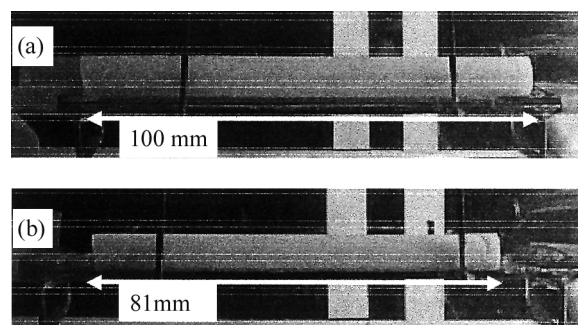


Fig. 2. Digital camera image used to monitor shrinkage of a boehmite sample dried at 50 °C, 50% RH, $v = 0.35$ m/s at a drying time: (a) $t_d = 0$ min; (b) $t_d = 240$ min.

combination of the varying pore structures, surface energy properties and the initial moisture content values.

3.1. Shrinkage

Fig. 2 illustrates the imaging results achieved using the digital camera for a boehmite sample at the start and the end of the shrinkage period.

The travelling microscope technique was limited in that only measurements of sample diameter and sample length were possible. Thus, the digital camera imaging technique was developed as a complimentary shrinkage measurement methodology. The imaging technique allowed shrinkage to be monitored in real time with the digital camera interfaced to an online computer. For the ceramic rod specimens, this shrinkage monitoring technique has proven to be as accurate as that using the travelling microscope with the added advantage that it allows 'shrinkage animations' to be generated. These 'shrinkage animations' illustrate frame-by-frame deformations, for example, bending or warping, that occur during the drying process. It is considered that this technique has the potential for monitoring the shrinkage of injection moulded ceramic components of complex geometry where the requirement for understanding processing deformations during drying are vital prior to binder burn-out and/or sintering in order to fulfil strict final product dimension specifications.

Fig. 3 illustrates the shrinkage curves of the major length dimension for the three ceramic materials investigated during drying under identical drying conditions. Both the travelling microscope and digital camera imaging techniques were used in order to acquire the shrinkage data and were found to be in good agreement. Shrinkage has been defined as the percentage ratio between the measured length (l) and the original length (l_0). The magnitude of the shrinkage observed is directly related to the initial moisture content (dry basis), X_0 , of the paste system. The critical moisture content, X_c , is defined as the moisture content at which shrinkage ceases. Table 1 summarises the shrinkage results obtained for the three ceramic paste systems.

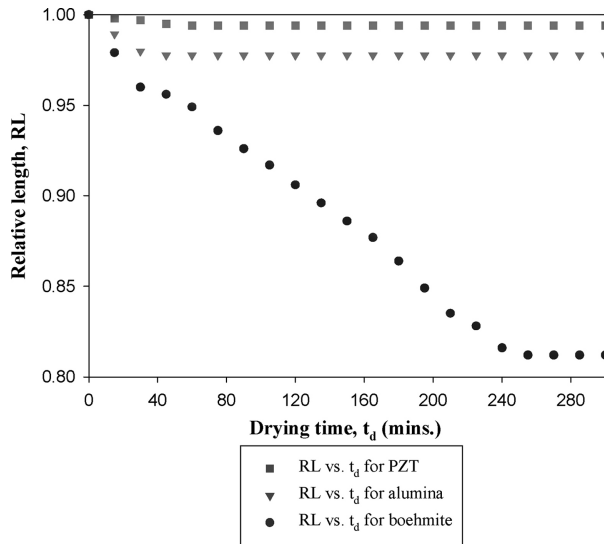


Fig. 3. Relative length vs. drying time for PZT, alumina and boehmitic rods all dried at 50°C, 50% RH, $v = 0.35$ m/s acquired using the travelling microscope shrinkage monitoring technique.

3.2. Alumina BAX 541

The main feature of the drying rate curve (Fig. 4) is the overall falling-rate type of behaviour. The initial moisture content of the alumina paste system tends towards the lower domain of values, $X_0 \approx 20\%$, as compared with the boehmite paste system, $X_0 \approx 100\%$. Alumina illustrates typical second falling-rate period (2FRP) behaviour. There is no evidence of a constant-rate period of drying. This observation is confirmed by the temperature data which indicates that the sample core temperature rises towards the dry-bulb thermometer temperature. This suggests that the alumina surface is not covered with a film of liquid and thus the liquid menisci of the partially filled pores are continuously receding into the ceramic body. During the 3FRP, the sharp rise in core temperature towards the dry-bulb temperature suggests that diffusion of moisture through the virtually empty pores is the rate controlling mechanism. Thus a combination of capillary flow and diffusive mechanisms control the rate of drying of alumina.

In order to establish the effectiveness of controlled drying, identical alumina rods were extruded and then allowed to dry on a bench in the laboratory and in the drying cabinet. Three different levels of relative humidity, 84, 50 and 31% RH, were employed for the controlled drying experiments.

Table 1
Summary of shrinkage results for Fig. 3

Ceramic paste system	X_0 (%)	X_c (%)	RL ($=l/l_0$)	Shrinkage (%)
PZT	8	7	0.99	1
Alumina	20	18	0.97	3
Boehmite	93	40	0.81	19

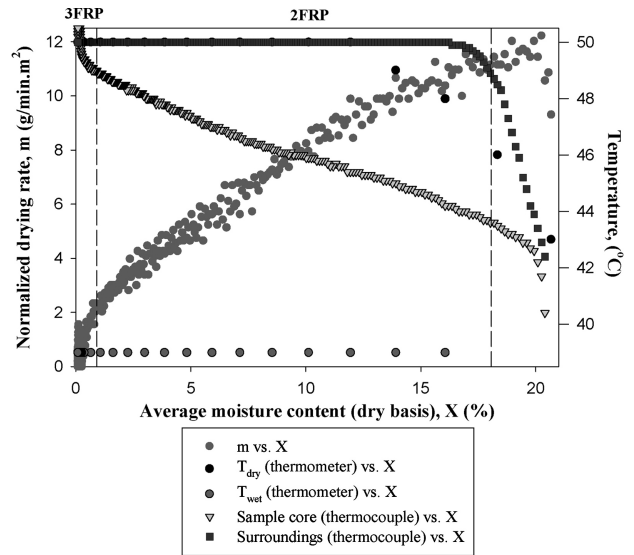


Fig. 4. Normalised drying rate and temperature profiles vs. average moisture content (dry basis) for a $d_0 = 6.5$ mm alumina BAX 541 rod dried in the horizontal plane at 50°C, 50% RH, $v = 0.35$ m/s.

The results illustrated in Fig. 5 show that the highest Weibull modulus was achieved at the lowest RH level. This may be a result of the particles packing closer together under more severe drying conditions, that is, at the highest drying rate. It is observed that there is a systematic increase in Weibull modulus with drying rate.

Table 2 lists the conditions of drying, the average bending strengths along with the sintered densities of the alumina samples.

The improvement in strength towards the low RH level is correlated to the increasing Weibull modulus. However, the Weibull modulus values are not as high as expected,

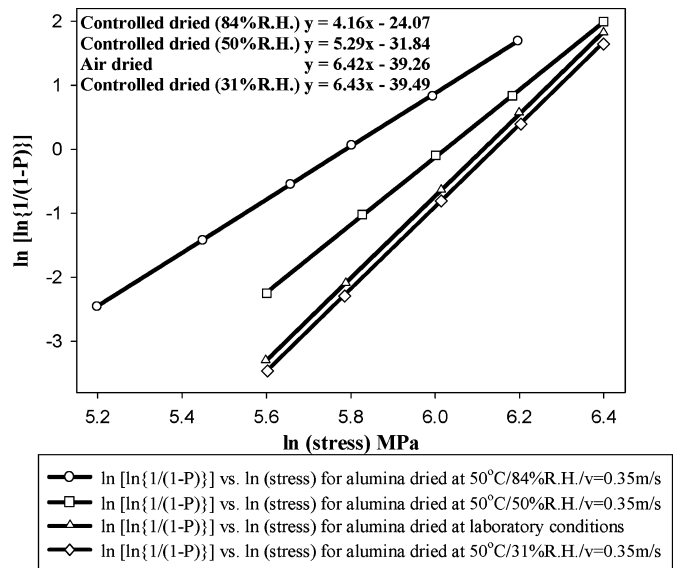


Fig. 5. Weibull modulus plot for $d_0 = 6.5$ mm alumina BAX 541 samples.

Table 2

Drying conditions (T and RH), average bending strengths (σ_{av}), sintered densities (ρ_{sint}) and percentage theoretical densities ($\% \rho_{theo}$) for alumina BAX 541 samples

T ($^{\circ}\text{C}$)	RH (%)	σ_{av} (MPa)	ρ_{sint} (kg/m^3)	$\% \rho_{theo}$ (%)
50	84	297.1	3761	94.7
50	50	380.6	3842	96.8
Air dried	Air dried	421.7	3870	97.5
50	31	432.8	3931	99.0

suggesting a scattering of defects within the material which are reflected in the low average bending strengths. Nevertheless, with the low RH level the alumina samples attained 99% theoretical density, that is $3970 \text{ kg}/\text{m}^3$. The polished fracture surface of the alumina specimens were examined in a scanning electron microscope (SEM) facility. It was found that the degree of macro-cracking was reduced under the lower operating RH level, thus corroborating the strength data.

3.3. Boehmite PURAL SB1

In order to demonstrate the effectiveness of controlled drying, a batch of at least 35 boehmite samples were dried under controlled conditions of relative humidity, temperature and convective air flow in the drying cabinet, and for comparison, an identical batch was dried on the bench in the laboratory. All of the samples possessed an initial diameter of 3.0 mm. Drying characteristics were determined for the specimens dried under controlled conditions (Fig. 6).

This drying rate curve indicates that three different periods of drying exist, they being: (i) a first falling-rate period (1FRP) associated with shrinkage of the ceramic;

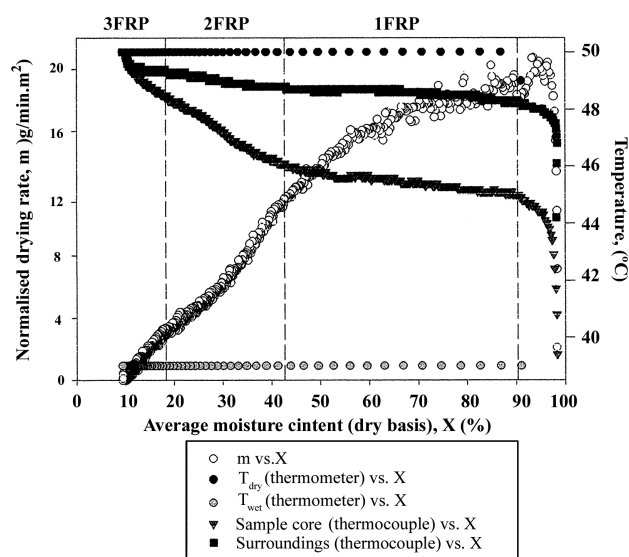


Fig. 6. Normalised drying rate and temperature profiles vs. average moisture content (dry basis) for a $d_0 = 3.0 \text{ mm}$ boehmite PURAL SB1 dried in the horizontal plane at 50°C , $50\% \text{ RH}$, $v = 0.35 \text{ m/s}$.

Table 3

Drying conditions (T and RH), average bending strengths (σ_{av}), sintered densities (ρ_{sint}) and percentage theoretical densities ($\% \rho_{theo}$) for boehmite PURAL SB1 samples

T ($^{\circ}\text{C}$)	RH (%)	σ_{av} (MPa)	ρ_{sint} (kg/m^3)	$\% \rho_{theo}$ (%)
Air dried	Air dried	108.2	3531	88.9
50	50	114.5	3652	92.0

(ii) a second falling-rate period (2FRP) in which the volume of the ceramic remains constant; (iii) a third falling-rate period (3FRP), where the rate of change of drying with respect to the change in moisture content remains constant.

In the case of boehmite, the 1FRP is associated predominantly with moisture transport up to the surface by capillary flow through the fine-pore structure of the material and the evaporation of moisture from the surface which is covered with a thin film of moisture. The onset of the 2FRP demonstrates a change in the functional form of the drying rate curve and occurs once shrinkage has ceased at $X \approx 43\%$. During the 2FRP, the sample core temperature rises rapidly ultimately attaining the value of the dry-bulb thermometer temperature (Fig. 6). The 2FRP is a combination of capillary flow and diffusion towards the surface. The 3FRP exhibits a further transformation in the functional form of the drying rate curve, which is also signified by the fact that the ceramic body attains the dry-bulb temperature. Once all the pores are empty, diffusion mechanisms increasingly control the drying rate down to the equilibrium moisture content of the dried material.

The controlled and uncontrolled drying average bending strength and sintered density results are shown in Table 3.

This particular boehmite paste mix is being developed for catalyst support applications where a porous microstructure is required and therefore it was not the aim of sintering to achieve full densification of $3970 \text{ kg}/\text{m}^3$ and thus the development of high strength was not expected. The low bending strength values suggest large defects which exist within a narrow range as reflected by the Weibull modulus values (Fig. 7). However, the controlled dried boehmite samples exhibited a marginally superior strength as compared to the air dried samples. Also, without alumina seeding, the controlled dried boehmite attained a higher density on sintering than in the case of the air dried batch. The more severe RH conditions within the environmental cabinet lead to an enhanced densified microstructure within the green body prior to sintering. In the case of the air dried samples, where the ambient conditions within the laboratory are subject to variation, the resulting physical properties were observed to be inferior to those of the controlled dried samples.

3.4. PZT 5A

The approximately linear functional form of the drying rate curve for PZT (Fig. 8) strongly suggests that diffusion is the major rate controlling drying mechanism. This

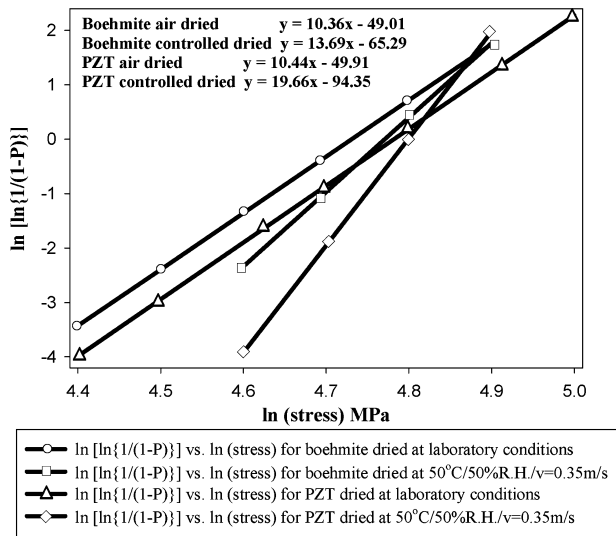


Fig. 7. Weibull modulus plots for $d_0 = 3.0$ mm boehmite PURAL SB1 and PZT 5A samples.

observation is verified by the sample temperature data illustrated in Fig. 8, which shows a rapid rise towards the dry-bulb temperature. Uncontrolled air drying leads to severe macro-cracking which thus prevented the PZT from being poled and thereby being endowed with piezoelectric properties.

However, controlled drying avoided macro-cracking and lead to the development of a structure with only a limited number of micro-pores thus facilitating successful poling.

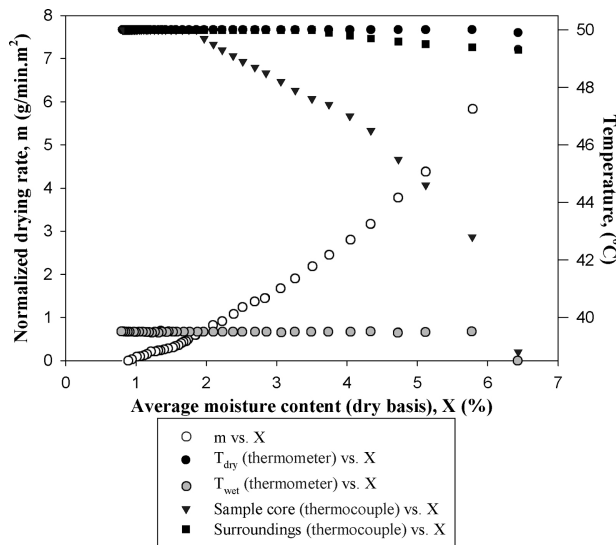


Fig. 8. Normalised drying rate and temperature profiles vs. average moisture content (dry basis) for a $d_0 = 3.0$ mm PZT 5A rod dried in the horizontal plane at 50°C , 50% RH, $v = 0.35$ m/s.

Table 4

Drying conditions (T and RH), average bending strengths (σ_{av}), sintered densities (ρ_{sint}) and percentage theoretical densities ($\% \rho_{theo}$) for PZT 5A samples

T ($^\circ\text{C}$)	RH (%)	σ_{av} (MPa)	ρ_{sint} (kg/m^3)	$\% \rho_{theo}$ (%)
Air dried	Air dried	113.9	7585	98.5
50	50	117.1	7690	99.9

The sintered densities, average bending strengths and drying conditions are given in Table 4.

It is clear that controlled drying does enhance the average bending strength values, the Weibull modulus (Fig. 7) and leads to 99.9% theoretical sintered density, that is 7690 kg/m^3 .

Once again, the effectiveness of controlled drying has been demonstrated, as in the cases of alumina and boehmite, to the extent that the PZT rods can be poled successfully thus fulfilling their functionality as piezoelectric components.

4. Conclusions

It has been demonstrated that the different ceramic materials possess unique drying characteristics with respect to drying rate, shrinkage and sample temperature behaviour.

The use of a non-intrusive drying system, together with digital camera monitoring, has been illustrated as an effective combination of experimental techniques in determining the drying characteristics of ceramic materials.

Controlled drying has been proven to enhance the physical and mechanical properties of a range of technical ceramics relative to their end use. The utility of this drying technique is especially apparent in the case of PZT, which only under controlled drying conditions facilitates poling and can thus be endowed with piezoelectric properties.

Acknowledgements

The authors would like to acknowledge the EPSRC for their financial support throughout this work.

References

- [1] R.K. Dwivedi, Drying behaviour of alumina gels, *J. Mater. Sci. Lett.* 5 (1986) 373–376.
- [2] I.P. Kilbride, A.J. Barker, The effect of sample dimensions on the drying behaviour and physical properties of extruded boehmite gels, *ICHEME Research Event Proceedings*, 1995, pp. 586–588.
- [3] D.H. Pearce, T.W. Button, Helical form piezoelectric macro-scale actuators, *Brit. Cer. Proceedings* 60 (1) (1999) 43–44.